Title	Voting rule optimisation for double threshold energy detector-based cognitive radio networks
Author(s)	Horgan, Donagh; Murphy, Colin C.
Publication date	2010-12
Original citation	Horgan, D.; Murphy, C. C (2010) Voting rule optimisation for double threshold energy detector-based cognitive radio networks. Signal Processing and Communication Systems (ICSPCS) Gold Coast, Queensland, Australia, 13-15 Dec 2010. IEEE
Type of publication	Conference item
Link to publisher's version	https://ieeexplore.ieee.org/xpl/login.jsp?tp=&arnumber=5709679 http://dx.doi.org/10.1109/ICSPCS.2010.5709679 Access to the full text of the published version may require a subscription.
Rights	**© 2010 IEEE. Personal use of this material is permitted. Permission from IEEE must be obtained for all other uses, in any current or future media, including reprinting/republishing this material for advertising or promotional purposes, creating new collective works, for resale or redistribution to servers or lists, or reuse of any copyrighted component of this work in other works.**
Item downloaded from	http://hdl.handle.net/10468/1044

Voting Rule Optimisation for Double Threshold Energy Detector-Based Cognitive Radio Networks

Donagh Horgan
Department of Electrical Engineering,
University College Cork,
Ireland
donaghh@rennes.ucc.ie

Colin C. Murphy
Department of Electrical Engineering,
University College Cork,
Ireland
cmurphy@rennes.ucc.ie

***Abstract*—The method by which individual decisions are combined in cooperative cognitive radio networks is crucial to minimising the overall probabilities of false alarm and missed detection. In this paper, general expressions for these probabilities are derived for a double threshold energy detector-based network, and an analytical solution for the optimal value of voting rule is found so that the overall probability of error is minimised.**

Simulation results show that there are significant advantages to the use of double threshold energy detector-based networks as opposed to their single threshold-based counterparts; additional simulations verify that the analytical solution is optimal.

I. INTRODUCTION

The electromagnetic spectrum is a valuable natural resource: without it, there would be no radio, television or mobile telephony services, not to mention the plethora of other applications for which it is employed. Like other natural resources, it is imperative that the electromagnetic spectrum is used responsibly, maximising its benefits for all.

Over the past few years, significant research has taken place in the area of spectrum utilisation. Worryingly, studies by the Federal Communications Commission [1], [2] and the National Telecommunications and Information Administration [3] indicate that the majority of the usable electromagnetic spectrum (i.e. bands with good propagation characteristics) has been licensed in the United States, leaving an ever-decreasing allocation for new applications.

A survey by the European Regulators Group [4] found that four EU member countries did not have the frequency resources available for additional 2G/3G mobile networks. This current lack of available spectrum resources does not bode well for future competition.

Fortunately, the problem is not intractable: statistics show that spectrum usage varies significantly depending on time and/or location [5]. To exploit this variation, an intelligent radio platform has been proposed [6]; it is envisaged that this new platform, known as Cognitive Radio, will have the ability to identify and broadcast in the unused areas of spectrum, thereby freeing up occupied frequency bands, while allowing existing and legacy systems to function as normal.

However, the technical challenges involved in designing such devices are many and complex. For example, in a licensed band, if the primary signal is not detected, the cognitive radio risks interfering with licensed broadcasts - this is an unacceptable situation for the primary user who may have paid a license fee for broadcast rights.

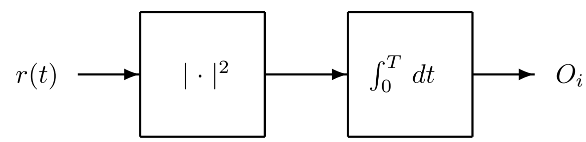

Fig. 1. Illustration of an energy detector.

One promising solution is for neighbouring cognitive radios to pool their resources in order to sense the licensed signals at very low power levels, thus ensuring a very low probability of interference. This approach, known as cooperative spectrum sensing, is quickly becoming a key candidate for next-generation wireless technologies.

In this paper, networks of cooperating double threshold energy detectors are considered. In particular, it is shown that the performance of such networks can be significantly greater than networks of cooperating single threshold detectors, even when there are fewer cooperating nodes. This increase in receiver sensitivity is a crucial step towards the realisation of efficient spectrum utilisation.

II. SYSTEM MODEL

A. Energy Detection

1) Single Threshold Detection: Energy detection is a spectrum sensing method consisting of a square law device and an integrator, as shown in Figure 1. Although it has been shown to have a higher sample complexity than other methods of spectrum sensing, such as matched filter detection or cyclostationary feature detection [7], it has a low implementation cost,t which makes it more commercially viable.

Each node in a cognitive radio network must decide whether the band of interest is occupied or not. The usual method of accomplishing this task is the binary hypothesis test (see Figure 2), where a decision is made based on discrete observations of the spectrum.

978-1-4244-7907-8/10/$26.00 2010 IEEE

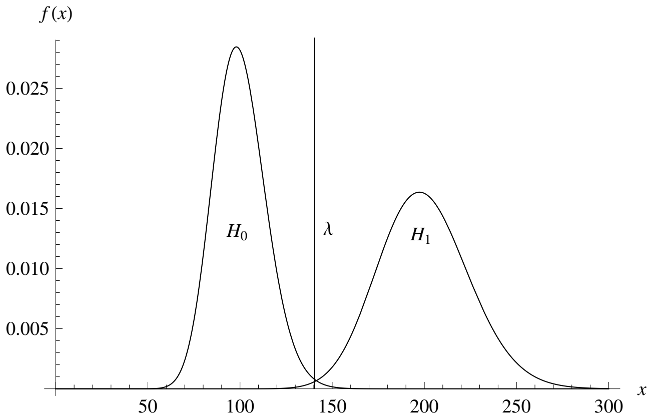

Fig. 2. Illustration of a binary hypothesis test with chi square (H_0) and noncentral chi square (H_1) probability density functions and single threshold λ.

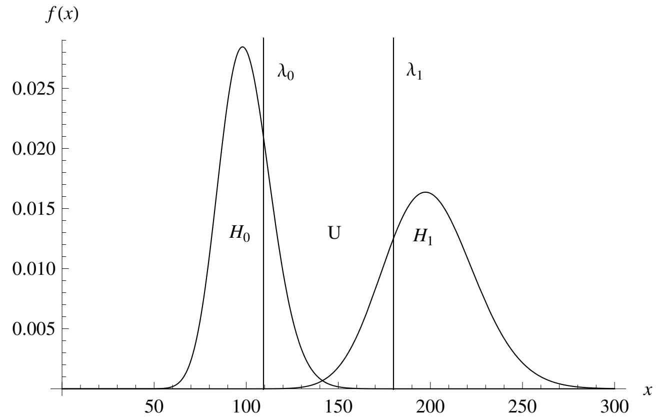

Fig. 3. Illustration of a hypothesis test with chi square (H_0) and noncentral chi square (H_1) probability density functions, lower threshold λ_0, upper threshold λ_1 and uncertainty region U.

In the typical case of a cognitive radio in a noisy environment, the received signal will be:

$$r(t) = \begin{cases} n(t) & H_0 \\ s(t) + n(t) & H_1 \end{cases} \tag{1}$$

where $r(t)$ represents the received signal, $n(t)$ represents time-varying noise interference, $s(t)$ represents the transmitted signal, and H_0 and H_1 represent the null and alternative hypotheses, respectively.

The energy detector operates by taking discrete samples of the spectrum and processing them to form a test statistic, which is then compared to a pre-calculated threshold. When the test statistic is less than the threshold, the null hypothesis is chosen; when it is greater, the alternative hypothesis is chosen, as per:

$$D_i = \begin{cases} H_0 & O_i < \lambda \\ H_1 & O_i \geq \lambda \end{cases} \tag{2}$$

where D_i is the decision at node i, O_i is the measured energy (i.e. the test statistic) at node i and λ is the threshold. It should be noted here that λ is assumed to be identical at each node.

Due to the square-law integrator process (see Figure 1), the distribution of the energy of the received signal at node i will be [8]:

$$O_i \sim \begin{cases} \chi^2_{2u} & H_0 \\ \chi^2_{2u}(2\gamma) & H_1 \end{cases} \tag{3}$$

where χ^2_{2u} and $\chi^2_{2u}(2\gamma)$ are the central and noncentral chi square distributions, respectively, u is the time-bandwidth product and γ is the noncentrality parameter. Again, it is assumed that these parameters are identical at each node.

In addition, the following relationships should be noted [8], [9, p. 45-47]:

$$u = \frac{N_s}{2} \tag{4}$$

$$\gamma = SNR \tag{5}$$

where N_s is the number of samples and SNR is the signal to noise ratio.

Energy detection is not a recent development, and its principles are well-understood [8], [10], [11]. In its simplest form, a single threshold is used, and the associated probabilities are defined as [8], [9], [12]:

$$\begin{aligned} P_f &= P(O_i > \lambda | H_0) \\ &= \frac{\Gamma(u, \frac{\lambda}{2\sigma^2})}{\Gamma(u)} \end{aligned} \tag{6}$$

$$\begin{aligned} P_a &= P(O_i \leq \lambda | H_0) \\ &= 1 - P_f \end{aligned} \tag{7}$$

$$\begin{aligned} P_d &= P(O_i > \lambda | H_1) \\ &= Q_u\left(\sqrt{\frac{2\gamma}{\sigma^2}}, \sqrt{\frac{\lambda}{\sigma^2}}\right) \end{aligned} \tag{8}$$

$$\begin{aligned} P_m &= P(O_i \leq \lambda | H_1) \\ &= 1 - P_d \end{aligned} \tag{9}$$

where P_f, P_a, P_d and P_m are the probabilities of false alarm, acquisition, detection and missed detection, respectively, σ^2 is the power of the noise signal $n(t)$ (assuming a 1Ω reference resistor), $\Gamma(a, b)$ is the upper incomplete gamma function, $\Gamma(a)$ is the gamma function and $Q_u(a, b)$ is the Marcum Q function.

2) Double Threshold Detection: The double threshold energy detector employs two thresholds which define the same hypotheses as the single threshold detector, in addition to a region of uncertainty where the detector chooses neither H_0 nor H_1 but, instead, reports that it is unsure which hypothesis is true (see Figure 3):

$$D_i = \begin{cases} H_0 & O_i < \lambda_0 \\ U & \lambda_0 \leq O_i < \lambda_1 \\ H_1 & O_i \geq \lambda_1 \end{cases} \tag{10}$$

where λ_0 and λ_1 are the lower and upper thresholds, respectively, and U is the decision representing uncertainty.

The use of two thresholds allows the probabilities of false alarm and missed detection to be set arbitrarily low at the cost of an increased uncertainty region; this is the principle on which double threshold energy detection relies.

The probabilities associated with the double threshold detector are defined as [13]:

$$\begin{aligned} P_f &= P(O_i > \lambda_1 | H_0) \\ &= \frac{\Gamma(u, \frac{\lambda_1}{2\sigma^2})}{\Gamma(u)} \end{aligned} \tag{11}$$

$$\begin{aligned} P_a &= P(O_i \leq \lambda_0 | H_0) \\ &= 1 - \frac{\Gamma(u, \frac{\lambda_0}{2\sigma^2})}{\Gamma(u)} \end{aligned} \tag{12}$$

$$\begin{aligned} \Delta_0 &= P(\lambda_0 < O_i \leq \lambda_1 | H_0) \\ &= 1 - P_f - P_a \end{aligned} \tag{13}$$

$$\begin{aligned} P_d &= P(O_i > \lambda_1 | H_1) \\ &= Q_u \left(\sqrt{\frac{2\gamma}{\sigma^2}}, \sqrt{\frac{\lambda_1}{\sigma^2}} \right) \end{aligned} \tag{14}$$

$$\begin{aligned} P_m &= P(O_i \leq \lambda_0 | H_1) \\ &= 1 - Q_u \left(\sqrt{\frac{2\gamma}{\sigma^2}}, \sqrt{\frac{\lambda_0}{\sigma^2}} \right) \end{aligned} \tag{15}$$

$$\begin{aligned} \Delta_1 &= P(\lambda_0 < O_i \leq \lambda_1 | H_1) \\ &= 1 - P_d - P_m \end{aligned} \tag{16}$$

where Δ_0 is the probability of uncertainty under H_0 and Δ_1 is the probability of uncertainty under H_1.

B. Cooperative Networks

1) Single Threshold Detection: Energy detection is not an ideal candidate for cognitive radio since it is a sub-optimal process [14], and has been shown to be susceptible to uncertainty in parameter measurements [7]. However, through the use of networks of individual detectors, significant performance gains can be achieved. Typically, this involves each detector node making an individual decision about spectrum occupancy; the decisions are then transmitted across a control channel (e.g. an underlay channel or a fixed frequency channel [14]) and processed either at a designated master node, or at a fixed control center.

In the case of single threshold energy detection, the decisions can be either H_0 or H_1 (see (2)). Each node transmits its decision to the fusion center where the votes for each hypothesis are counted and an overall decision is made, based on a pre-defined voting rule. Generally, the k-out-of-N rule is used [15]:

$$D_{fc} = \begin{cases} H_0 & \sum_{i=1}^{N} g(D_i) < k \\ H_1 & \sum_{i=1}^{N} g(D_i) \geq k \end{cases} \tag{17}$$

where D_{fc} is the decision at the fusion center, N is the total number of nodes in the network, k is the voting rule, and the function $g(\cdot)$ is defined as:

$$g(D_i) = \begin{cases} 0 & D_i \neq H_1 \\ 1 & D_i = H_1. \end{cases} \tag{18}$$

The associated probabilities for the k-out-of-N rule for a single threshold detector network are [13], [15]:

$$Q_f = \sum_{l=k}^{N} \binom{N}{l} P_a^{N-l} P_f^l \tag{19}$$

$$Q_a = 1 - Q_f \tag{20}$$

$$Q_d = \sum_{l=k}^{N} \binom{N}{l} P_m^{N-l} P_d^l \tag{21}$$

$$Q_m = 1 - Q_d \tag{22}$$

where Q_f, Q_a, Q_d and Q_m are the overall probabilities of false alarm, acquisition, detection and missed detection, respectively.

2) Double Threshold Detection: For the double threshold energy detector, there are three possible decisions: H_0, H_1 and U. This allows for a greater degree of flexibility with the counting process as the number of uncertain nodes can change with each poll of the network (with a single threshold detector there are no uncertain nodes since there is no uncertainty region). Thus, by setting the area (i.e. the probability) of the uncertainty region appropriately, it is possible to censor the decisions of the nodes most likely to make erroneous decisions, as shown in Figure 3.

It should be noted that the fusion center decision rule for a double threshold energy detector-based network is the same as for a single threshold network (see (17)).

Previous to this work, to the best of the authors' knowledge, no general equations existed in the literature for describing the relevant probabilities for a double threshold detector network with an arbitrary voting rule. The overall probability of false alarm is given by (see Appendix A for proof):

$$Q_f = \frac{\sum_{l=k}^{K} \binom{K}{l} P_a^{K-l} P_f^l}{(1 - \Delta_0)^K}, \tag{23}$$

where K is the number of certain nodes (i.e. the number of nodes that choose either H_0 or H_1). Applying a similar process, the following equation can be derived for the overall probability of detection:

$$Q_d = \frac{\sum_{l=k}^{K} \binom{K}{l} P_m^{K-l} P_d^l}{(1-\Delta_1)^K}. \quad (24)$$

As before, the overall probabilities of acquisition and missed detection are defined as:

$$Q_a = 1 - Q_f, \quad (25)$$

$$Q_m = 1 - Q_d. \quad (26)$$

III. Voting Rule Optimisation

In previous work [15], the optimal voting rule (i.e. the voting rule minimising the overall probability of error) for a single threshold detector network was found to be:

$$k_{opt} = \left\lceil \frac{N \log\left(\frac{P_a}{P_m}\right)}{\log\left(\frac{P_d P_a}{P_f P_m}\right)} \right\rceil \quad (27)$$

where k_{opt} is the optimal voting rule and $\lceil \cdot \rceil$ is the ceiling function.

To find the optimal voting rule for a double threshold detector network, it is necessary to define:

$$\begin{aligned} G(k) &= Q_f + Q_m \\ &= 1 + \sum_{l=k}^{K} \binom{K}{l} \left(\frac{P_a^{K-l} P_f^l}{(1-\Delta_0)^K} - \frac{P_m^{K-l} P_d^l}{(1-\Delta_1)^K} \right) \end{aligned} \quad (28)$$

where $G(k)$ is the error function.

$G(k)$ can be either maximised or minimised by finding the solution of:

$$\left. \frac{dG(k)}{dk} \right|_{k=k_{opt}} = 0. \quad (29)$$

The second derivative test can then be applied to determine whether this solution is a maximum or a minimum.

Noting that k is integer, the following simplification can be made:

$$\begin{aligned} \frac{dG(k)}{dk} &\approx \frac{G(k+1) - G(k)}{(k+1) - (k)} \\ &= \binom{K}{k} \left(\frac{P_m^{K-k} P_d^k}{(1-\Delta_1)^K} - \frac{P_a^{K-k} P_f^k}{(1-\Delta_0)^K} \right). \end{aligned} \quad (30)$$

Solving (29) for k_{opt} yields the following (see Appendix B for proof):

$$k_{opt} = \left\lceil \frac{K \log\left(\frac{P_a(1-\Delta_1)}{P_m(1-\Delta_0)}\right)}{\log\left(\frac{P_d P_a}{P_f P_m}\right)} \right\rceil. \quad (31)$$

It should be noted that k_{opt} satisfies $1 \leq k_{opt} \leq K$ since the probability of error is unity outside this range. In the case where $K = N$ (i.e. $\Delta_0 \to 0$, $\Delta_1 \to 0$), (31) simplifies to (27).

IV. Simulation Results

A. Voting Rule Optimality

In order to assess the accuracy of (31), a simulation was carried out where the lower threshold was varied while the signal to noise ratio, number of samples and threshold separation ($\lambda_1 - \lambda_0$) were kept constant. As can be seen in Figure 4, the analytical solution matches the optimum voting rule found via simulation across the whole range of values.

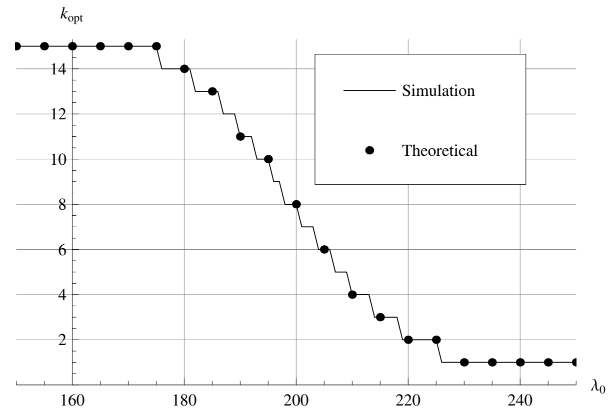

Fig. 4. Plot of optimal voting rule against lower threshold value for a network of 20 nodes, 15 of which are certain, with $SNR = -10dB$, $N_s = 200$, $\lambda_1 = \lambda_0 + 20$.

B. Performance: Best Case Scenario

To quantify the maximum performance of double threshold detection, a best case scenario was analysed. Here, both the single and double threshold detector networks have twenty nodes, and each double threshold detector node is certain, i.e. all twenty nodes vote H_0 or H_1. As can be seen in Figure 5, the value of the error function at the optimal voting rule for a double threshold network is lower than at the optimal voting rule for a single threshold network.

In the case where both networks are utilising their respective optimal voting rules, it can be seen (Figure 8) that the double threshold detector network outperforms the single threshold detector network in terms of receiver sensitivity. Specifically, given an overall error probability of 0.05, the double threshold detector network outperforms the single threshold by a margin of almost 2dB.

C. Performance: Practical Scenarios

In a more practical scenario, several cognitive radio nodes are likely to report that they are uncertain. Unsurprisingly, this increases the overall probability of error for the double threshold detector network. However, it is still possible for the double threshold network to outperform the single threshold network, as shown in Figure 6, but only when the number of reporting nodes is sufficiently large.

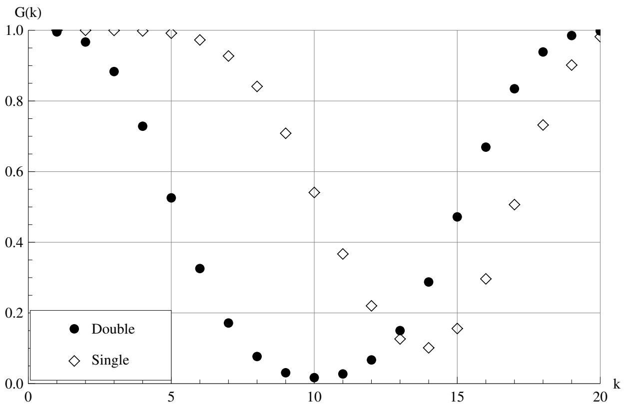

Fig. 5. Plot of the error function against voting rule for a network of 20 nodes, all of which are certain, with $SNR = -10dB$, $N_s = 200$, $\lambda = \lambda_0 = 200$, $\lambda_1 = 220$.

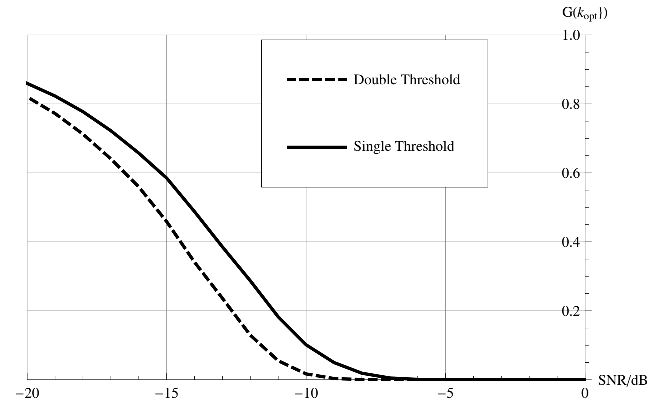

Fig. 8. Plot of the error function with optimised voting rule against SNR for a network of 20 nodes, all of which are certain, with $N_s = 200$, $\lambda = \lambda_0 = 200$, $\lambda_1 = 220$.

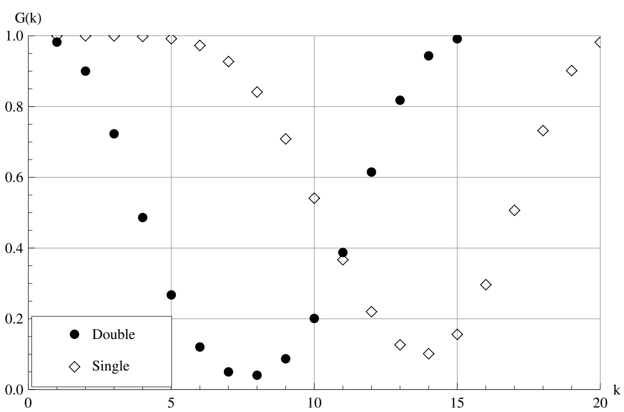

Fig. 6. Plot of the error function against voting rule for a network of 20 nodes, 15 of which are certain, with $SNR = -10dB$, $N_s = 200$, $\lambda = \lambda_0 = 200$, $\lambda_1 = 220$.

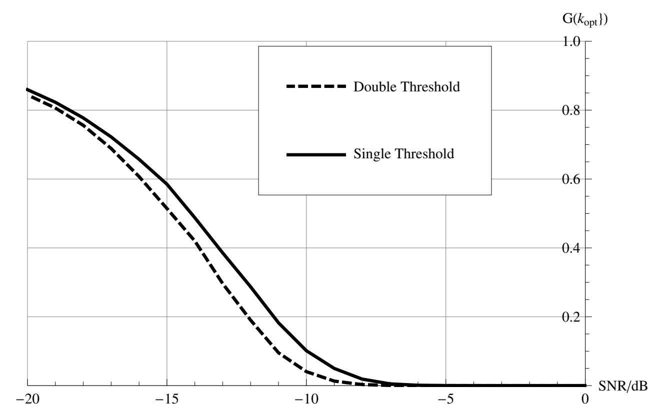

Fig. 9. Plot of the error function with optimised voting rule against SNR for a network of 20 nodes, 15 of which are certain, with $N_s = 200$, $\lambda = \lambda_0 = 200$, $\lambda_1 = 220$.

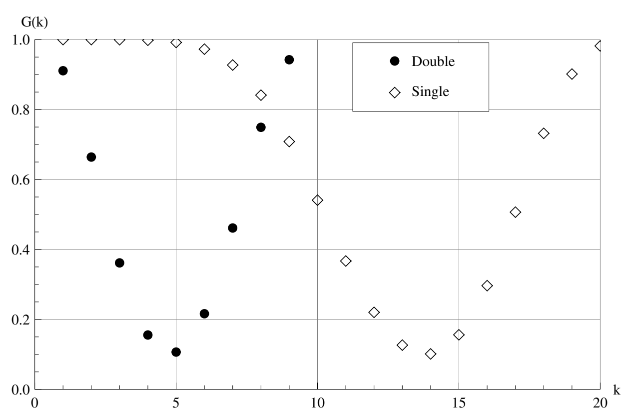

Fig. 7. Plot of the error function against voting rule for a network of 20 nodes, 9 of which are certain, with $SNR = -10dB$, $N_s = 200$, $\lambda = \lambda_0 = 200$, $\lambda_1 = 220$.

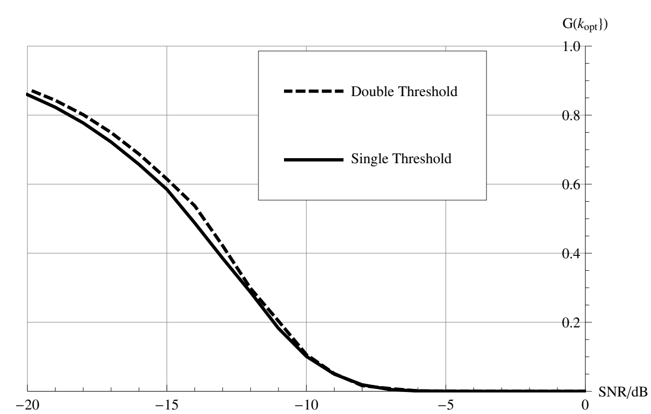

Fig. 10. Plot of the error function with optimised voting rule against SNR for a network of 20 nodes, 9 of which are certain, with $N_s = 200$, $\lambda = \lambda_0 = 200$, $\lambda_1 = 220$.

In the case where the number of reporting nodes is too small, in this instance when fewer than ten nodes vote (see Figure 7), the single threshold detector network begins to outperform the double threshold detector network. However, it should be noted that the number of uncertain nodes is proportional to the area of the uncertainty region itself, and so such a scenario could only occur if the thresholds had been placed in such a way that the uncertainty region was large; this situation is always avoidable as the placement of thresholds, as far as this work is concerned, is flexible.

Figures 9 and 10 illustrate the effect of increasing the number of uncertain nodes on receiver sensitivity. In the case where fifteen out of twenty nodes are certain, the double threshold detector network outperforms the single threshold detector network; in the case where nine out of twenty are certain, the single threshold detector network begins to outperform the double threshold detector network.

V. Conclusion

In this paper, general expressions for the probabilities of error for a double threshold energy detector-based network with arbitrary voting rule and unknown number of certain nodes were derived. These expressions were simplified for the practical case where the number of certain nodes is known at the fusion center at the time of decision fusion, and an expression for the optimal voting rule in this case was derived.

Simulation results showed that the derived equation for the optimal voting rule matches the actual optimal voting rule across a range of values. In addition, it was shown that the correct choice of voting rule is crucial to minimising the overall probability of error and that no one rule is optimal for all situations.

Simulation results also illustrated how the number of certain nodes, and by extension, the size of the uncertainty region, is crucial to the performance of the double threshold scheme. A combined optimal threshold placement and optimal voting rule selection scheme would be desirable to find the performance limits of both single and double threshold-based networks - only then could a real comparison be made between the limits of both techniques. It is envisaged that this will be the focus of future work.

Appendix A
Derivation of double threshold energy detector network probabilities

For both single and double threshold energy detectors, the network probability of false alarm is defined as:

$$\begin{aligned} Q_f &= P(D_{fc} = H_1 | H_0) \\ &= \frac{P((D_{fc} = H_1) \cap H_0)}{P(H_0)} \end{aligned} \tag{32}$$

where $P(H_0)$ is the probability of an event occurring from the set of events H_0.

H_0 consists entirely of false alarm and acquisition events, and both subsets are mutually exclusive as false alarms and acquisitions cannot occur simultaneously, by definition. Thus:

$$\begin{aligned} P(H_0) =& P((D_{fc} = H_0) \cap H_0) \\ &+ P((D_{fc} = H_1) \cap H_0). \end{aligned} \tag{33}$$

To simplify notation, it is convenient to define F as the set of false alarm events and A as the set of acquisition events:

$$P(F) = P((D_{fc} = H_1) \cap H_0) \tag{34}$$

$$P(A) = P((D_{fc} = H_0) \cap H_0) \tag{35}$$

where $P(F)$ and $P(A)$ are the probabilities of an event occurring from the sets of events F and A, respectively. Now, combining (32), (33), (34) and (35):

$$Q_f = \frac{P(F)}{P(A) + P(F)}. \tag{36}$$

For a single threshold detector, $P(F)$ and $P(A)$ are binomially distributed [15]:

$$P(F) = \sum_{l=k}^{N} \binom{N}{l} P_a^{N-l} P_f^l \tag{37}$$

$$P(A) = \sum_{l=0}^{k-1} \binom{N}{l} P_a^{N-l} P_f^l \tag{38}$$

where the lower index for $P(F)$ (i.e. $l = k$) is determined by the decision rule specified in (17). Summing $P(A)$ and $P(F)$:

$$\begin{aligned} P(A) + P(F) &= \sum_{l=0}^{k-1} \binom{N}{l} P_a^{N-l} P_f^l + \sum_{l=k}^{N} \binom{N}{l} P_a^{N-l} P_f^l \\ &= \sum_{l=0}^{N} \binom{N}{l} P_a^{N-l} P_f^l \\ &= 1. \end{aligned} \tag{39}$$

This is easily verifiable using the binomial theorem and the relationship:

$$P_f = 1 - P_a. \tag{40}$$

Now, combining (36), (37) and (39):

$$Q_f = \sum_{l=k}^{N} \binom{N}{l} P_a^{N-l} P_f^l.$$

A similar process can be applied to show that (21) holds true.

For the double threshold detector network, both $P(F)$ and $P(A)$ change due to the uncertainty region:

$$P(F) = \sum_{l=k}^{N} \binom{N}{l} \sum_{K=l}^{N} \binom{N-l}{K-l} P_a^{K-l} P_f^l \Delta_0^{N-K} \tag{41}$$

$$P(A) = \sum_{l=0}^{k-1} \binom{N}{l} \sum_{K=l}^{N} \binom{N-l}{K-l} P_a^{K-l} P_f^l \Delta_0^{N-K}. \tag{42}$$

These equations are analogous to (37) and (38); the additional binomial distribution describes the relationship between the probability of acquisition and the probability of uncertainty.

In this case, the summation of $P(A)$ and $P(F)$ is:

$$\begin{aligned}P(A)+P(F)=&\sum_{l=0}^{k-1}\binom{N}{l}\sum_{K=l}^{N}\binom{N-l}{K-l}P_a^{K-l}P_f^l\Delta_0^{N-K}\\&+\sum_{l=k}^{N}\binom{N}{l}\sum_{K=l}^{N}\binom{N-l}{K-l}P_a^{K-l}P_f^l\Delta_0^{N-K}\\=&\sum_{l=0}^{N}\binom{N}{l}\sum_{K=l}^{N}\binom{N-l}{K-l}P_a^{K-l}P_f^l\Delta_0^{N-K}\\=&1.\end{aligned}\tag{43}$$

This can be verified using the binomial theorem and the relationship:

$$\Delta_0 = 1 - P_a - P_f. \tag{44}$$

Now, combining (36), (41) and (43):

$$Q_f = \sum_{l=k}^{N}\binom{N}{l}\sum_{K=l}^{N}\binom{N-l}{K-l}P_a^{K-l}P_f^l\Delta_0^{N-K}. \tag{45}$$

Equation (45) represents the overall probability of false alarm given a voting rule, k, and unknown number of certain nodes, K. However, at the fusion center, the number of certain nodes is always known prior to any summation of results, and so it is possible to simplify:

$$P(F) = \sum_{l=k}^{N}\binom{N}{l}\binom{N-l}{K-l}P_a^{K-l}P_f^l\Delta_0^{N-K},$$

$$P(A) = \sum_{l=0}^{k-1}\binom{N}{l}\binom{N-l}{K-l}P_a^{K-l}P_f^l\Delta_0^{N-K}. \tag{46}$$

Noting that:

$$\binom{N}{l}\binom{N-l}{K-l} = \binom{N}{K}\binom{K}{l}, \tag{47}$$

it is possible to simplify further:

$$P(F) = \binom{N}{K}\Delta_0^{N-K}\sum_{l=k}^{K}\binom{K}{l}P_a^{K-l}P_f^l, \tag{48}$$

$$P(A) = \binom{N}{K}\Delta_0^{N-K}\sum_{l=0}^{k-1}\binom{K}{l}P_a^{K-l}P_f^l. \tag{49}$$

Thus, the summation becomes:

$$\begin{aligned}P(A)+P(F)=&\binom{N}{K}\Delta_0^{N-K}\sum_{l=0}^{K}\binom{K}{l}P_a^{K-l}P_f^l\\=&\binom{N}{K}\Delta_0^{N-K}(1-\Delta_0)^K.\end{aligned}\tag{50}$$

Again, this can be verified by applying the binomial theorem.

Now, combining (36), (48) and (50):

$$\begin{aligned}Q_f &= \frac{\binom{N}{K}\Delta_0^{N-K}\sum_{l=k}^{K}\binom{K}{l}P_a^{K-l}P_f^l}{\binom{N}{K}\Delta_0^{N-K}(1-\Delta_0)^K}\\&= \frac{\sum_{l=k}^{K}\binom{K}{l}P_a^{K-l}P_f^l}{(1-\Delta_0)^K}.\end{aligned}\tag{51}$$

In the case where K equals N (i.e. $\Delta_0 \to 0$), both (45) and (51) simplify to (19).

A similar process can be applied to show that (24) is true.

Appendix B
Derivation of optimal voting rule

To find the optimal voting rule, it is necessary to find the solution to:

$$\binom{K}{k_{opt}}\left(\frac{P_m^{K-k_{opt}}P_d^{k_{opt}}}{(1-\Delta_1)^K} - \frac{P_a^{K-k_{opt}}P_f^{k_{opt}}}{1-\Delta_0)^K}\right) = 0. \tag{52}$$

Solving this for k_{opt}:

$$k_{opt} = \frac{K\log\left(\frac{P_a(1-\Delta_1)}{P_m(1-\Delta_0)}\right)}{\log\left(\frac{P_dP_a}{P_fP_m}\right)}. \tag{53}$$

This may produce a non-integer value; however, the overall probabilities of false alarm and missed detection are binomially distributed, and so, by definition, the ceiling function must be applied. Thus, the true optimal voting rule is:

$$k_{opt} = \left\lceil \frac{K\log\left(\frac{P_a(1-\Delta_1)}{P_m(1-\Delta_0)}\right)}{\log\left(\frac{P_dP_a}{P_fP_m}\right)} \right\rceil. \tag{54}$$

By the second derivative test, for (54) to minimise the overall probability of error, it must be shown that:

$$\left.\frac{d^2G(k)}{dk^2}\right|_{k=k_{opt}} > 0. \tag{55}$$

Again, because k is an integer, the following simplification can be made:

$$\frac{d^2G(k)}{dk^2} = \frac{\frac{dG(k+1)}{dk} - \frac{dG(k)}{dk}}{(k+1)-(k)}. \tag{56}$$

Now, using (29):

$$\begin{aligned}\left.\frac{d^2G(k)}{dk^2}\right|_{k=k_{opt}} =&\left.\frac{dG(k+1)}{dk}\right|_{k=k_{opt}} - \left.\frac{dG(k)}{dk}\right|_{k=k_{opt}}\\=&\left.\frac{dG(k+1)}{dk}\right|_{k=k_{opt}} - 0.\end{aligned}\tag{57}$$

Thus, it must be shown that:

$$\binom{K}{k_{opt}+1}\left(\frac{P_m^{K-k_{opt}-1}P_d^{k_{opt}+1}}{(1-\Delta_1)^K}-\frac{P_a^{K-k_{opt}-1}P_f^{k_{opt}+1}}{(1-\Delta_0)^K}\right)>0. \tag{58}$$

Simplifying this:

$$\frac{P_d}{P_m}\frac{P_m^{K-k_{opt}}P_d^{k_{opt}}}{(1-\Delta_1)^K}-\frac{P_f}{P_a}\frac{P_a^{K-k_{opt}}P_f^{k_{opt}}}{(1-\Delta_0)^K}>0. \tag{59}$$

Now, recalling (52), it suffices to show that:

$$\frac{P_d}{P_m}-\frac{P_f}{P_a}>0$$
$$P_dP_a>P_mP_f. \tag{60}$$

This will always be true as $P_d > P_m$ and $P_a > P_f$ by design. Thus, (54) will minimise the overall probability of error.

ACKNOWLEDGEMENTS

This work was funded by the Irish Research Council for Science, Education and Technology (IRCSET) through the Embark Initiative.

REFERENCES

[1] FCC, "FCC Spectrum Inventory Table," 1996. [Online]. Available: http://www.fcc.gov/oet/info/database/spectrum/spinvtbl.pdf

[2] ——, "FCC Adopts Rules for Unlicensed Use of Television White Spaces," Nov. 2008. [Online]. Available: http://hraunfoss.fcc.gov/edocs_public/attachmatch/FCC-08-260A1.pdf

[3] NTIA, "NTIA Frequency Allocation Chart," 2003. [Online]. Available: http://www.ntia.doc.gov/osmhome/allochrt.pdf

[4] European Regulators Group, "ERG Complementary Report on Possible Bottlenecks in Mobile Access"," 2006. [Online]. Available: http://erg.eu.int/doc/publications/erg_06_45_b_complementary_report_on_possible_bottlenecks_in_mobile_access.pdf

[5] M. A. McHenry and K. Steadman, "Spectrum Occupancy Measurements, Location 1 of 6: Riverbend Park, Great Falls, Virginia, Tech. Rep." The University of Kansas Center for Research, Inc., Riverbend Park, Great Falls, Virginia, Tech. Rep. 1, Apr. 2004. [Online]. Available: http://www.sharedspectrum.com/inc/content/measurements/nsf/1_NSF_Riverbend_Park_Report.pdf

[6] J. Mitola and G. Maguire, "Cognitive Radio: Making Software Radios More Personal," *Personal Communications, IEEE*, vol. 6, no. 4, pp. 13–18, 1999.

[7] R. Tandra, "Fundamental Limits on Detection in Low SNR," Masters of Science in Engineering, University of California, Berkeley, 2005.

[8] H. Urkowitz, "Energy Detection of Unknown Deterministic Signals," *Proceedings of the IEEE*, vol. 55, no. 4, pp. 523–531, 1967.

[9] J. G. Proakis and M. Salehi, *Digital Communications*. McGraw-Hill, Jan. 2008.

[10] D. Slepian, "Some Comments on the Detection of Gaussian Signals in Gaussian Noise," *Information Theory, IRE Transactions on*, vol. 4, no. 2, pp. 65–68, 1958.

[11] D. Middleton, "On the Detection of Stochastic Signals in Additive Normal Noise–I," *Information Theory, IRE Transactions on*, vol. 3, no. 2, pp. 86–121, 1957.

[12] A. Nuttall, "Some Integrals Involving the Qm Function," *Information Theory, IEEE Transactions on*, vol. 21, no. 1, pp. 95–96, 1975.

[13] J. Zhu, Z. Xu, F. Wang, B. Huang, and B. Zhang, "Double Threshold Energy Detection of Cooperative Spectrum Sensing in Cognitive Radio," in *Cognitive Radio Oriented Wireless Networks and Communications, 2008. CrownCom 2008. 3rd International Conference on*, 2008, pp. 1–5.

[14] D. Cabric, S. Mishra, and R. Brodersen, "Implementation Issues in Spectrum Sensing for Cognitive Radios," in *Signals, Systems and Computers, 2004. Conference Record of the Thirty-Eighth Asilomar Conference on*, vol. 1, 2004, pp. 772–776 Vol.1.

[15] W. Zhang, R. Mallik, and K. Letaief, "Optimization of Cooperative Spectrum Sensing with Energy Detection in Cognitive Radio Networks," *Wireless Communications, IEEE Transactions on*, vol. 8, no. 12, pp. 5761–5766, 2009.